Available online at www.sciencedirect.com
ScienceDirect
International Journal of Thermal Sciences 47 (2008) 1–6
International Journal of Thermal Sciences
www.elsevier.com/locate/ijts

Estimation of the effective thermal conductivity of carbon felts used as PEMFC Gas Diffusion Layers

Julien Ramousse *, Sophie Didierjean, Olivier Lottin, Denis Maillet

Laboratoire d'Energétique et de Mécanique Théorique et Appliquée, UMR 7563 CNRS–INPL–UHP, 2, avenue de la forêt de Haye, BP 160, 54504 Vandoeuvre lès Nancy Cedex, France

Received 6 September 2006; received in revised form 11 January 2007; accepted 11 January 2007

Available online 23 February 2007

Abstract

Thermal conductivity of gas diffusion layers (GDL) used in fuel cells is a key parameter for the analysis of heat transfer in membrane electrodes assembly (MEA). In this paper, we focus on non-woven carbon felts. Although correlations are available, the felts thermal conductivity is difficult to estimate due to the nature of heat transfer in porous and fibrous materials: the effective conductivity of the solid phase is roughly known and the correlations giving effective conductivity of porous media (solid and fluid phases) have restricted range of application. Consequently, we chose to associate an analytical and an experimental approach. Their results converge and clearly show that the majority of values encountered in the literature are, most probably, highly overestimated.

Keywords: PEM fuel cell; Gas Diffusion Layer; Carbon felt; Effective thermal conductivity; Thermal resistance; Experimental approach

1. Introduction

The modelling of heat transfer in a proton exchange membrane fuel cell requires the knowledge of the thermal properties of each element. A review of the literature shows that thermal conductivity of Nafion membrane is pretty well known (Table 1) whereas the thermal conductivity of Gas Diffusion Layers (GDLs) is more difficult to estimate. The porosity of the GDLs makes it necessary to use effective thermal conductivities for describing heat transfer in the solid and fluid phases [1]. In addition to having high porosities, the GDLs are also anisotropic, which is probably the reason why thermal conductivity values encountered in the literature are so dispersed (Table 2). Most of the results reported in Tables 1 and 2 are estimated from the thermal conductivities of each phase and their volumetric fraction in the medium. Only the values proposed by Vie and Kjelstrup [2] come from experimental temperature measurement in a running fuel cell. The present paper is directly relevant to the recent published work of Kandelwal and Mench [7]. They achieve ex situ experimental measurements of the through-plane thermal conductivity of varying fuel cell components, including the electrolyte, catalyst layer and diffusion media. Starting from this report, we tried to estimate the GDLs conductivity as well as possible, theoretically and experimentally.

Table 1
Effective thermal conductivities of the dry membrane—review

Parameter	Value	Ref.
k_{eff} (W m^{-1} K^{-1})	0.455	[3]
	0.43	[4]
	0.34	[5]
	0.21	[6]
	0.18	[2]
	0.16 ± 0.03 at 20 °C 0.13 ± 0.02 at 65 °C	[7]
	0.14	[8]
	0.1 ± 0.1	[2]

The nature and structure of GDLs is described in the next section. Then, the analytical model of Danes and Bardon [9] and other correlations of the literature [10] are used to estimate their effective thermal conductivity. The results are compared

* Corresponding author. Tel.: +33 (0) 3 83 59 56 19; fax: +33 (0) 3 83 59 55 31.
E-mail address: julien.ramousse@ensem.inpl-nancy.fr (J. Ramousse).

1290-0729/$ – see front matter
doi:10.1016/j.ijthermalsci.2007.01.018

Nomenclature

a	contact radius between fibres	m
b	mean fibre radius	m
Cp	specific heat capacity	$J\,kg^{-1}\,K^{-1}$
g	gravity acceleration	$m\,s^{-2}$
Gr	Grashof number	
k	thermal conductivity	$W\,m^{-1}\,K^{-1}$
L	thickness	m
n	number of layers	
P	pressure	bar
Pe	Peclet number	
R	thermal resistance	$K\,W^{-1}$ or $K\,m^{-2}\,W^{-1}$
S	surface	m^2
T	temperature	K
U	fibres tangle ratio	
v	velocity	$m\,s^{-1}$

Greek letters

α	constriction ratio	
β	thermal dilation coefficient	K^{-1}
ε	porosity or volumetric fraction	
φ	thermal flux	$W\,m^{-2}$
μ	viscosity	$kg\,m^{-1}\,s^{-1}$
ρ	density	$kg\,m^{-3}$
τ	tortuosity	

Subscripts

device	with the device
eff	effective (thermal conductivity)
f	fluid phase or function
fibre	fibre
gas	gas
layers	between layers
m	medium
s	solid phase
tot	total

Superscripts

Max	maximum
MXW	Maxwell model
Min	minimum
$\perp$	in the transversal direction
$\parallel$	in the longitudinal direction
c	contact (resistance)

Table 2
Effective thermal conductivities of the GDL—review

Parameter	Value	Ref.
k_{eff} ($W\,m^{-1}\,K^{-1}$)	65	[4]
	30	[6]
	21.5	[11]
	1.6	[5,12]
	1.6	[13]
	1.3	[3]
	0.5; 1; 2.94	[14]
	1.8 ± 0.27 at 26 °C 1.24 ± 0.19 at 73 °C	[7]
	0.2 ± 0.1	[2]

to experimental values obtained from different samples of non-woven commercial GDL.

2. Structure

Experiments were carried out for different *Quintech* and *SGL Carbon* GDLs, of thicknesses ranging from 190 to 480 μm. Their structure was observed by Scanning Electron Microscopy (Figs. 1 and 2). Samples of *Quintech* and *SGL Carbon* felts show the same structure: the porous matrix consists of unordered but coplanar carbon fibres (about 7 μm in diameter) and the void fraction is significant, the porosity being estimated by the manufacturer to 80% [13]. However, it should be noted that *Quintech* GDL fibres are straight whereas *SGL Carbon* GDL fibres are curved. This difference in shape, probably due to manufacturing processes, should imply variations in the GDL effective thermal conductivity [9]. From the pictures in Fig. 1, it is possible to distinguish PTFE (PolyTetraFluoroEthylene) deposited on the *SGL Carbon* felt, making it hydrophobic. There is no PTFE in the *Quintech* GDL in Fig. 1.

3. Theoretical approach

The aim of this section is to discuss the theoretical value of carbon felts effective thermal conductivity, starting from the knowledge of solid and fluid properties.

3.1. Solid phase

The structure of felts is at the origin of difficulties in estimating the thermal conductivity of the solid phase [9]: fibres orientation implies anisotropic thermal behaviour, with a much higher conductivity parallel to the felt than in the transverse direction. Indeed, if thermal resistance parallel to the plane is mainly of conductive nature, thermal resistance in the transverse direction depends mostly on the quality of contact between fibres. In addition, the fibres themselves can be anisotropic, mainly because of the structure of graphite: the carbon atoms form adjacent hexagonal cells forming one atom thick layers. Among the three allotropes of carbon (graphite, diamond and fullerenes or nanotubes), only diamond is thermally isotropic. Danes and Bardon [9] assumes that heat transfer occurs mostly along the fibres: consequently, their model does not require the knowledge of fibres radial conductivity. In this paper, the axial thermal conductivity of carbon fibres is considered equal to the value generally attributed to dense graphite: $k_{fibre} = 120\ W\,m^{-1}\,K^{-1}$.

The model of Danes and Bardon allows the calculation of felt thermal conductivity according to parameters such as the

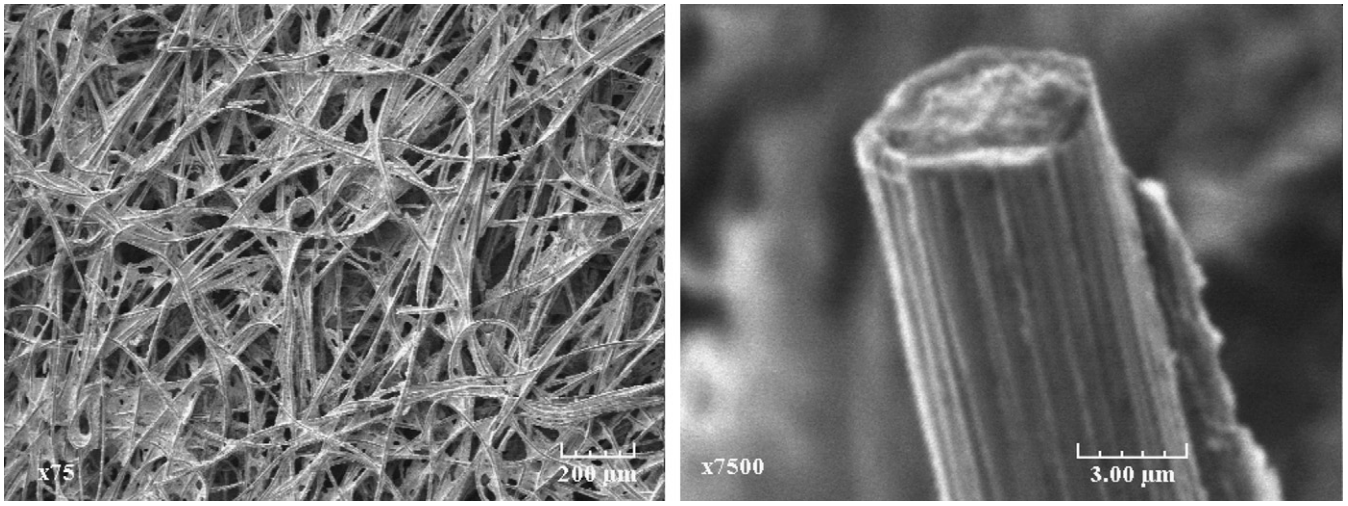

Fig. 1. Structure of *SGL Carbon* sample.

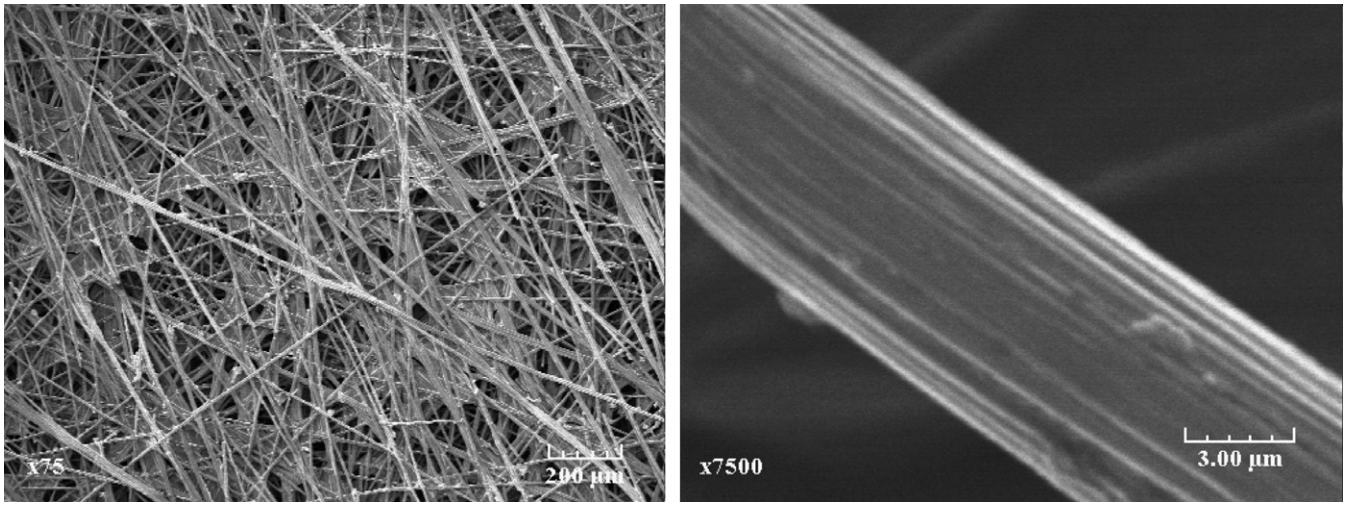

Fig. 2. Structure of *Quintech* sample (190 µm thick).

tortuosity τ, the fibres tangle ratio U and the contact radius a between two fibres.

The tangle ratio is defined as the average percentage of fibres that are not strictly coplanar to the GDL (thus improving heat transfer in the through-plane direction). The contact radius a (apparent radius of the contact disk between two cylindrical fibres) makes it possible to define the constriction ratio $\alpha = a/b$, where b is the mean fibre radius.

The thermal conductivities of the solid matrix respectively in the transverse ($k_s^{\perp}$) and longitudinal ($k_s^{\parallel}$) directions are given by:

$$k_s^{\perp} = f(k_{\text{fibre}}, \varepsilon, \tau, U, \alpha) \quad \text{and} \quad k_s^{\parallel} = \frac{1-\varepsilon}{2\tau^2} k_s^{\perp} \tag{1}$$

However, most of these parameters are difficult to evaluate and we are only able to estimate a possible range for the felt effective thermal conductivity. In Table 3, two sets of parameters are considered, amongst which the porosity (0.8) and the fibres axial conductivity (120 $\mathrm{W\,m^{-1}\,K^{-1}}$) are kept constant. The second set of parameters yields transverse and longitudinal conductivities significantly higher, only because of a different arrangement of fibres. As expected, the effective thermal conductivity is lower in the transverse direction than in the direction parallel to the plan ($k_s^{\perp} < k_s^{\parallel}$). Similarly, the transverse conductivity is more affected by changes in τ, U and α than the longitudinal conductivity. For both structures, the values are 1 or 2 orders of magnitude lower than the fibre axial conductivity.

Table 3
Analytical estimation of the solid phase effective thermal conductivity (parallel to the plan and transverse) of the solid phase, according to the model of Danes and Bardon [13]

Parameter	Structure 1	Structure 2
	Values	
k_{fibre} ($\mathrm{W\,m^{-1}\,K^{-1}}$)	120	120
ε (–)	0.8	0.8
τ (–)	1,7	1
U (–)	5%	20%
α (–)	1%	3%
$k_s^{\parallel}$ ($\mathrm{W\,m^{-1}\,K^{-1}}$)	4.15	12
$k_s^{\perp}$ ($\mathrm{W\,m^{-1}\,K^{-1}}$)	0.21	1.39

3.2. Effective thermal conductivity of the fibre matrix saturated with a fluid (gas)

Heat flux in the GDL does not depend only on the solid phase, but also on the fluid phase occupying the pores, with a contribution combining conductive and convective heat transfer.

- In the absence of external forces, the importance of the natural convection can be estimated by means of the *Grashof* number, interpreted as the ratio of buoyancy forces to viscous forces:

$$Gr = \frac{\rho\beta g L^3 \Delta T}{\mu} \tag{2}$$

  It is possible to over-estimate *Grashof* number by maximizing the GDLs thickness and neglecting the solid phase: considering a 500 μm layer of air separating two isothermal planes whose temperatures differ by 5 K gives a result lower than 0.1. Consequently, one can affirm that natural convection is negligible in PEM fuel cell GDLs.
- During fuel cell operation, the gaseous reactants and products flow through the Gas Diffusion Layer. The *Peclet* number (*Pe*) quantifies the importance of advection with respect to diffusion. According to results presented in a previous work [15] ($v_{gas} \propto 10^{-3}$ m s^{-1}), the maximum value of *Pe* is lower than 0.01 for the same length L as above, even at the highest current densities, showing that convective heat transfer can be neglected compared to conductive heat transfer.

$$Pe = \frac{(\rho Cp)_{gas} v_{gas} L}{k_{gas}} \tag{3}$$

According to these last two results, conduction is the most important contribution to heat transfer in the fluid phase. Many correlations allow estimating the effective thermal conductivity of a porous medium starting from those of the two phases. The simplest are obtained by connecting in series or in parallel the thermal resistances associated with both phases [10]. These models yield to the lowest (k_{eff}^{Max}: series) and highest (k_{eff}^{Min}: parallel) values of effective thermal conductivity, respectively:

$$k_{eff}^{Max} = \sum_i \varepsilon_i k_i \tag{4}$$

$$\frac{1}{k_{eff}^{Min}} = \sum_i \frac{\varepsilon_i}{k_i} \tag{5}$$

The Maxwell model [16] yields another estimate of the effective thermal conductivity:

$$k_{eff}^{MXW} = \frac{k_s[(1-\varepsilon)(2k_s + k_f) + 3\varepsilon k_f]}{(1-\varepsilon)(2k_s + k_f) + 3\varepsilon k_s} \tag{6}$$

The thermal conductivities of pure fluids (at $T = 80\,^{\circ}$C and $P = 1$ bar) are reported in Table 4, starting from Eqs. (4) to (6), estimates of the effective conductivity of GDL saturated with air are given in Table 5. The results are much lower than most of the values reported in Table 1. For instance, some authors [11] obtained 21.5 W m^{-1} K^{-1} using Maxwell model with $\varepsilon = 0.8$ and $k_s = 150.6$ W m^{-1} K^{-1}.

Table 4
Fluid thermal conductivities at $T = 80\,^{\circ}$C and $P = 1$ bar

Fluid	Thermal conductivity k (W m^{-1} K^{-1})
H_2	0.206
O_2	0.0307
N_2	0.0295
Air	0.03
H_2O_{vap}	0.0246
H_2O_{liq}	0.67

Table 5
Carbon felts effective thermal conductivity at $T = 80\,^{\circ}$C and $P = 1$ bar estimated with the values of k_s given in Table 3

	Structure 1			Structure 2		
	k_{eff}^{Min}	k_{eff}^{MXW}	k_{eff}^{Max}	k_{eff}^{Min}	k_{eff}^{MXW}	k_{eff}^{Max}
	Eq. (5)	Eq. (6)	Eq. (4)	Eq. (5)	Eq. (6)	Eq. (4)
k_{eff} (W m^{-1} K^{-1})	0.036	0.057	0.066	0.037	0.23	0.3

This section points out the difficulties in estimating the effective thermal conductivity of a porous and fibrous medium: the conductivity of the solid phase is roughly known and the correlations giving the solid and fluid effective thermal conductivity have restricted range of application. The influence of all parameters and the anisotropy of the medium cannot be described by simple models: the experimental determination remains the most efficient method for a precise evaluation of the thermal properties.

4. Measurements

4.1. Experimental set-up

Transient techniques like the flash method are not well adapted for characterizing thermal properties of thin media if they are semi-transparent. The only way of measuring thermal conductivity in steady state consists in setting a unidirectional heat flux φ_m inside the sample and measuring the temperature difference between both faces ΔT [17]. The total thermal resistance is given then by:

$$R_{tot} = \frac{\Delta T}{\varphi} \tag{7}$$

The samples are sandwiched between two copper plates (Fig. 3). The high thermal diffusivity of copper ensures a uniform temperature distribution and the temperature is measured with thermocouples located at the centre of the plates. Two fluxmeters (Peltier elements) [18] are placed on both sides of the sample-copper assembly. They measure the thermal flux imposed by the heating and cooling devices. A similar method is used by Khandelwal and Mench [7] to measure the equivalent thermal conductivity of various fuel cell components. Any small difference between the fluxes measured at the top (warm) and at the bottom (cold) can be easily explained by lateral convective losses. In order to limit these lateral convective losses produced

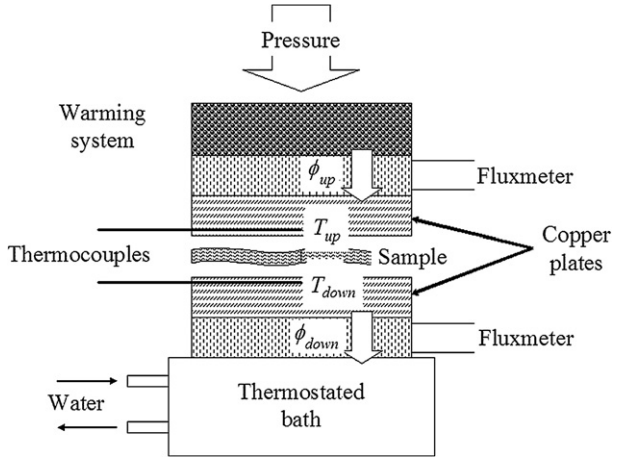

Fig. 3. Experimental set-up.

by air motion, the experimental set-up is kept under a bell-glass and the cooling and heating devices maintain the temperature of the sample close to the ambient (20 °C). According to Batsale and Degiovanni [17] the heat losses stay below 5% provided that the ratio between the sample thickness and its conductivity remains in the 1×10^{-3} and 2×10^{-2} K m^2 W^{-1} range. The mean value of the heat flux φ is used for calculating the thermal conductivity. The samples have a square section of 16 cm^2 and their thickness is carefully controlled.

4.2. Results

The measured thermal resistance R_{tot} is the sum of the sample thermal resistance R_{m} and of contact resistances with the copper plates $R^{\text{c}}_{\text{device}}$ so that:

$$R_{\text{tot}} = R_{\text{m}} + 2R^{\text{c}}_{\text{device}} \tag{8}$$

The thermal resistance of the sample is a function of its effective thermal conductivity k:

$$R_{\text{m}} = \frac{L}{kS} \tag{9}$$

Where S and L are the sample section and thickness.

Usually, the material thermal conductivity and the contact resistances are evaluated by testing samples of different thickness L_1 and L_2:

$$R^1_{\text{tot}} = \frac{L_1}{kS} + 2R^{\text{c}}_{\text{device}} \quad \text{and} \quad R^2_{\text{tot}} = \frac{L_2}{kS} + 2R^{\text{c}}_{\text{device}}$$
$$\text{then } k = \frac{L_1 - L_2}{S(R^1_{\text{tot}} - R^2_{\text{tot}})} \tag{10}$$

However, the thermal conductivity of carbon felts cannot be evaluated that way: as it will be highlighted later, the porous structure varies with the material thickness probably because of manufacturing processes. Consequently, tests were carried out with a stack of n identical samples (with n varying from 1 to 4). In this case, R_{tot} depends also on the additional contact resistances between layers $R^{\text{c}}_{\text{layers}}$. The total resistance R_{tot} is then expressed by:

$$R_{\text{tot}} = nR_{\text{m}} + (n-1)R^{\text{c}}_{\text{layers}} + 2R^{\text{c}}_{\text{device}} \tag{11}$$

The increase in the total resistance with the number of layers corresponds to the sum of material resistance R_{m} and contact resistance $R^{\text{c}}_{\text{layers}}$:

$$\frac{\Delta R_{\text{tot}}}{\Delta n} = R_{\text{m}} + R^{\text{c}}_{\text{layers}} = R_{\text{measured}} \tag{12}$$

The averaged values of R_{measured} are given in Table 6. The direct determination of $R^{\text{c}}_{\text{layers}}$ and R_{m} being impossible, the following assumptions are made:

- If the contact resistance $R^{\text{c}}_{\text{layers}}$ is neglected, the total resistance is fully attributed to the conductive resistance of the material, which is thus overestimated, giving the lower bound of the felt conductivity.
- Since the fibre diameter is about 7 μm, it is reasonable to think that the contact resistance $R^{\text{c}}_{\text{layers}}$ is lower than the resistance of a 10 μm thick air layer (0.24 K W^{-1}). This gives the upper bound of the felt conductivity.

The minimum and maximum values of different GDLs effective thermal conductivity are given in Table 6.

4.3. Discussion

Our measured values of carbon GDLs effective thermal conductivity are much lower than the majority of the estimates encountered in the literature (Table 2). Although carbon fibres are highly conductive, their orientation mostly perpendicular to the GDL and to the heat flux results in a low effective thermal conductivity. However, they are close to the analytical results presented in the previous section (Table 5, Structure 2). The measured values are slightly higher than the results of the models but these discrepancies are not surprising considering the difficulties in modelling heat transfer in porous media. They are also above those determined experimentally by Khandelwal and Mench [7]: possible material treatments and variation in different experimental conditions can explain these deviations.

Table 6
Estimated thermal conductivities of GDL samples at 20 °C. The dispersion is the averaged relative difference between the linear relation defined by Eqs. (11) and (12) and the experimental results

Sample ($A = 16$ cm^2)	R_{measured} (K W^{-1})	Dispersion (%)	$R^{\text{Max}}_{\text{m}}$ (K m^2 W^{-1})	$k^{\text{Min}}_{\text{eff}}$ (W m^{-1} K^{-1})	$R^{\text{Min}}_{\text{m}}$ (K m^2 W^{-1})	$k^{\text{Max}}_{\text{eff}}$ (W m^{-1} K^{-1})
Quintech (190 μm)	0.327	4.8	5.23E−04	0.36	1.39E−04	1.36
Quintech (280 μm)	0.537	4.3	8.59E−04	0.33	4.75E−04	0.59
Quintech (230 μm)	0.727	0.8	1.16E−03	0.20	7.79E−04	0.30
SGL Carbon (420 μm)	1.008	0.03	1.61E−03	0.26	1.23E−03	0.34

Our results must be compared to those obtained by Vie and Kjelstrup [2] (Table 2) starting from temperature measurements in a fuel cell under operation. According to them, the effective thermal conductivity of *ETEK*® GDL is $k_{\mathrm{ETEK}} = 0.2 \pm 0.1$ $\mathrm{W\,m^{-1}\,K^{-1}}$, which is of the same order as our experimental and analytical results. This tends to confirm that most of the values used in the literature are highly overestimated.

Thermal resistance of GDLs are not only linked to the material's thickness: one can notice that the thermal resistance of 190 and 280 μm *Quintech* samples are very close while they should differ by about 50% if their porous structure (and consequently, their effective thermal conductivity) were identical: this shows the influence of manufacturing processes on GDL effective thermal conductivity.

Two of the four tested samples are treated with PTFE (*Quintech* 230 μm and *SGL Carbon*). The thermal conductivity of PTFE is close to 0.23 $\mathrm{W\,m^{-1}\,K^{-1}}$ [10]. This additional material seems to reduce slightly the GDL effective conductivity but because of a lack of accurate information about the hydrophobic treatment, no definite conclusion can be drawn. However, these results are in agreement with the trend observed in [7].

Inside a fuel cell, the GDLs are saturated with humidified hydrogen (at the anode) and humidified air (at the cathode). As shown in Table 4, hydrogen has a higher thermal conductivity than air (2×10^{-1} $\mathrm{W\,m^{-1}\,K^{-1}}$ [10]), which can imply a small increase in the apparent conductivity (compared to our results). Similarly, the GDLs thermal conductivity would be higher if liquid water ($k_{\mathrm{H_2O_{liq}}} = 0.67$ $\mathrm{W\,m^{-1}\,K^{-1}}$ [10]) is present. A possible improvement of our experimental set-up would be to perform measurements under controlled atmosphere. Thus it would be possible to observe the variations in the thermal conductivity as a function of gas properties.

In fuel cells, the GDLs are compressed between the membrane and the bipolar plates, which should increase their effective thermal conductivity by improving contact between fibres and reducing porosity. However, the pressure to which the GDLs are submitted are difficult to evaluate, all the more so because it varies with membrane hydration. One way to address this issue would be to carry out in situ pressure or temperature measurements.

5. Conclusion

The effective thermal conductivity of carbon felts used as gas diffusion layers (GDLs) in fuel cells is much lower than the thermal conductivity of pure carbon because fibres arrangement in the felt induces important constriction resistances and contact resistances. Thus, the values of the effective thermal conductivity estimated and measured in this work are lower by one order of magnitude (at least) than most values of the literature. This difference can have significant consequences for fuel cell thermal management: in particular, the temperature difference between electrodes and bipolar plates could get higher than what is usually reported, which would limit condensation at the electrodes.

These results also show that the GDLs thermal conductivity is highly orthotropic: thermal gradients in the plane of the cell should be reduced thanks to a higher heat transfer than in the transverse direction.

References

[1] C. Moyne, S. Didierjean, H.P. Amaral Souto, O.T. da Silveira, Thermal dispersion in porous media: one-equation model, International Journal of Heat and Mass Transfer 43 (2000) 3853–3867.
[2] P.J.S. Vie, S. Kjelstrup, Thermal conductivities from temperature profiles in the polymer electrolyte fuel cell, Electrochemica Acta 49 (2004) 1069–1077.
[3] P.T. Nguyen, T. Berning, N. Djilali, Computational model of a PEM fuel cell with serpentine gas flow channels, Journal of Power Sources 130 (2004) 149–157.
[4] M. Wöhr, K. Bolwin, W. Schnurnberger, M. Fischer, W. Neubrand, G. Eigenberger, Dynamic modelling and simulation of a polymer membrane fuel cell including mass transport limitation, International Journal of Hydrogen Energy 23 (3) (1998) 213–218.
[5] A. Rowe, X. Li, Mathematical modelling of proton exchange membrane fuel cells, Journal of Power Sources 102 (12) (2001) 82–96.
[6] G. Maggio, V. Recupero, C. Mantegazza, Modelling of temperature distribution in a solid polymer fuel cell stack, Journal of Power Sources 62 (1996) 167–174.
[7] M. Khandelwal, M.M. Mench, Direct measurement of through-plane thermal conductivity and contact resistance in fuel cell materials, Journal of Power Sources 161 (2006) 1106–1115.
[8] W.-M. Yan, F. Chen, H.-Y. Wu, C.-Y. Soong, H.-S. Chu, Analysis of thermal and water management with temperature-dependent diffusion effects in membrane of proton exchange membrane fuel cells, Journal of Power Sources 129 (2004) 127–137.
[9] F. Danes, J.-P. Bardon, Conductivité thermique des feutres de carbone, isolants à forte anisotropie : modèle de conduction par la phase solide, Revue Générale de Thermique 36 (1997) 302–311.
[10] J. Taine, J.-P. Petit, Transferts thermiques—Mécanique des fluides anisothermes, Dunod Université, 1989.
[11] V. Gurau, H. Liu, S. Kakaç, Two-dimensional model for proton exchange membrane fuel cells, AIChE Journal 44 (11) (1998) 2410–2422.
[12] N. Djilali, D. Lu, Influence of heat transfer on gas and water transport in fuel cells, International Journal of Thermal Sciences 41 (2002) 29–40.
[13] Toray Industries Inc., Toray carbon paper, Toray Industries Inc., Advanced Composites Department, 2001.
[14] H. Ju, H. Meng, C.-Y. Wang, A single-phase, non isothermal model for PEM fuel cells, International Journal of Heat and Mass Transfer 48 (2005) 1303–1315.
[15] J. Ramousse, J. Deseure, S. Didierjean, O. Lottin, D. Maillet, Modelling of heat, mass and charge transfers in a PEMFC single cell, Journal of Power Sources 145 (2005) 416–427.
[16] J.C. Maxwell, A Treatise on Electricity and Magnetism, Clarendon Press, 1892.
[17] J.C. Batsale, A. Degiovanni, Mesure de résistance thermique de plaques minces à l'aide d'une mini-plaque chaude, Revue Générale de Thermique (1994).
[18] L. Dumont, C. Moyne, A. Degiovanni, Thermal contact resistance: experiment vs theory, International Journal of Thermophysics 19 (6) (1998) 1681–1690.